Investigation of the Blockage Correction to Improve the Accuracy of Taylor's Low-Speed Wind Tunnel

Journal of Physics: Conference Series **2222** (2022) 012008 doi:10.1088/1742-6596/2222/1/012008

Investigation of the Blockage Correction to Improve the Accuracy of Taylor's Low-Speed Wind Tunnel

A S M Al-Obaidi* and Ganesh Madivaanan

School of Computer Science and Engineering, Taylor's University, Malaysia

*Corresponding author: abdulkareem.mahdi@taylors.edu.my

Abstract. Placing a test model in the wind tunnel test section creates an interaction between the flow and the model and walls of the test section. This interaction affects the accuracy of data reading of the wind tunnel. One of the significant factors is the blockage which affects the drag and lift coefficients, causing inaccurate readings. This paper considered streamlined and blunted shapes of different sizes to investigate and assess the effect of the shape and size of the test model on the reading accuracy. Wind tunnel tests were conducted with the three different sizes for each shape to determine the aerodynamic coefficients of the models. Different correction methods were applied to find the correction coefficient. CFD simulations were performed using ANSYS Fluent software. A comparison of numerical and experimental results was carried out to determine the most suitable blockage correction method for the chosen models. It is found that a blockage ratio of less than 16% has the least blockage effect. The blockage correction of drag reduction for these models is very minimal, less than 1%. Correction coefficients for both shapes were derived to correct the blockage effect created by models with a blockage ratio of 16% or higher.

1. Introduction

Wind tunnels are simple experimental aerodynamics equipment that allows researchers to study the wind flow around a test model and the forces created and acting on the model, and their interactions with the flow of the wind tunnel's wind [1]. A wind tunnel aims to obtain aerodynamic data such as force and momentum coefficients, test various configurations, look at high lift devices, reduce drag, and develop simulators before the first flight [2]. Multiple industries, from aerospace to automobile, from wind turbines to shipbuilding, use wind tunnels to test various kinds of shapes and sizes of prototypes before the products are out in the market. When the models are being tested in the tunnel, aerodynamicists have to cautiously supervise the conditions of the flow, which influences the forces acting on the aircraft. By making careful force assessments and evaluations on the model, one can calculate and predict the number of forces that will act on a real scale aircraft.

Wind tunnels are designed with a specific purpose and with a specific speed range. There are numerous types of wind tunnels and model instrumentation available. Generally, wind tunnels are classified based on the speed range reached in the test section such as low-speed wind tunnel, high-speed wind tunnel, supersonic wind tunnel, and hypersonic wind tunnel [2]. Taylor's University owns an inbuilt wind tunnel that is used for various educational and research purposes. The wind tunnel in Taylor's University is an open circuit, low-speed subsonic wind tunnel, which is called Taylor's Low-Speed Wind Tunnel. Taylor's wind tunnel has rectangular test sections with a cross-section of 0.303 m by 0.303 m and a length of 0.885 m. The fan speed of a 3HP, 415 V/50 Hz, 0.63 m in diameter fan can be changed from 3.33 m/s to 38.35 m/s to

adjust the test section speed (KRUGER L06-RQ). With a Mach number ranging from 0 to 0.1, the TLWT fan can produce subsonic flow [3]. The open section wind tunnel is built with multiple sections, which are settling chamber with multiple screen arrangement, construction cone, test section, diffuser, and blower [4].

Testing a prototype in a wind tunnel has its advantages. When a field test is being conducted, it takes much less time and costs cheaper than testing with a real model. Furthermore, test parameters and boundaries in wind tunnels can be carefully monitored, allowing experiments and tests to be carried out at varying wind speeds and with low levels of turbulence intensity [5]. As much as it has advantages, wind tunnel testing also carries a few disadvantages. One of the disadvantages is that due to its small size, actual size prototypes cannot be tested. Instead, reduced-scale models were used. This would distort the test data because valid test readings can only be obtained by testing an actual model.

Another drawback is the wind tunnel test section's limited size. When a scale model is being tested and studied in wind tunnels, the test section's walls normally are nearer to the model than any other barrier that may be present in real-world operating conditions [5]. So, any models that are being tested in the test section are being tested in a constrained area. Unfavourably, these boundaries of the wind tunnel test section enact a restriction of flows that pass through any models that are being tested. Until now, a plethora of studies and researches have been done on this phenomenon, but it could not be fully understood [6]. The effects of the wind tunnel walls on the flows over a model can be classified in blockage, streamlined curvature, and buoyancy [6].

This research paper mainly focuses on the blockage effect and blockage correction method for Taylor's Low-Speed Wind Tunnel (TLWT). The blockage effects generated by the walls of wind tunnels are one of the most serious issues involved with wind tunnel testing [7]. Solid blockage and wake blockage are two types of blockage effects. In the current study, the blockage correction method was determined by comparing the experimental method and numerical method results. Experimental method results were collected through wind tunnel tests, while numerical method results were collected through CFD simulations.

2. Literature Review

Literature review analyses and discusses findings critically from different authors through their research papers. Their works would provide a better understanding of the project and contribute directly to the project. Each author briefly introduced the research subject in the first five sections, and the scope and findings were discussed in the following sections. Though the selected articles are used in the literature review, some publications do not provide enough information about the study's scope, technique, or boundary conditions. Finally, the literature review was summarised to conclude the finding for the scopes and methods of this project according to the literature review.

2.1. Overview of Blockage Effects

Whenever a scale model is being examined and studied in wind tunnels, the walls of the test section of wind tunnels are normally nearer to the model than any other barrier that may be present in real-world operating conditions [5]. So, any models that are being tested in the test section are being tested in a constrained area, where the test models are very near to the walls of the test section where it can cause serious blockage related issues. The blockage effect can distort reading such as drag and lifts coefficients. The effects of the wind tunnel walls on the flows over a model can be classified in blockage, streamlined curvature, and buoyancy [6]. This project will mainly focus on the blockage effect and blockage correction method for TWLT. The blockage effects generated by the walls of the wind tunnels are one of the most serious issues involved with wind tunnel testing [7]. As mentioned earlier, there are two types of blockage effects which are solid blockage and wake blockage. In the literature, there is no specific agreement on what the minimum blockage ratio should be, over which blockage correction is required. Blockage correction is likely to be

important in many open test-section wind tunnels for testing models, regardless of the minimum limit, with the necessity to adjust for blockage when the blockage ratio is in the range of 3-10 per cent and bigger.

2.2. Blockage Factor and Blockage Ratio

2.2.1. Blockage Factor

Blockage factor is defined as the ratio of the empty test section's wind speed to the test model's wind speed. The blockage factor is important when identifying the correction method because the blockage factor's initial power coefficient cube can be multiplied to adjust the power coefficient [5]. The blockage factor can be calculated as in equation (1):

$$B_F = \frac{U_t}{U_f} \tag{1}$$

where U_t is the tunnel wind speed with the model(m/s) and U_f is the tunnel wind speed without the model (m/s). The blockage factor is an excellent measure of how the wind speed varies because of blockage effects.

2.2.2. Blockage Ratio

The blockage ratio (BR) is defined as the ratio of the projected area of the model and the test section of the wind tunnel. The magnitude of the blockage effect on the drag coefficient was even significant at 5% of the blockage ratio. When the blockage ratio is increased, the absolute value of backpressure is found to increase. This directly caused the increase in the drag coefficient. A study made by Takeda and Kato [8] also reveals that in the test with a blockage ratio of less than 5%, there are no major blockage effects. Bigger sizes where the blockage ratios are higher would cause some difference in the wind tunnel measurement. This is due to the freestream's velocity increase and big drops in the pressure. Test conducted by Jeong et al. [5] prove that any wind tunnel test that has a blockage ratio higher than 10% must undergo a correction method.

2.3. Blockage Correction

When testing a model in an open wind tunnel, the test subject will take up a portion of the cross-sectional space of the wind tunnel. Because of the walls in the wind tunnel, the flow around the object will behave differently than it would outside in the open air. This is known as the blockage effect, and it must be considered while taking measurements in a closed wind tunnel. The equation was proposed by Maskell [9],

$$\frac{Cdu}{Cdc} = 1 + \Theta C_{du}\, BR \tag{2}$$

where C_{du} represents the uncorrected coefficient, C_{dc} is the corrected drag coefficient and Θ is the blockage constant. The base pressure coefficient and the aspect ratio determine the blockage constant, which is an empirical constant. The blockage constant for airfoil wings is estimated to be $\Theta = 0.9$ and for blunt shapes is estimated to be $\Theta = 0.96$ [10]. The adjusted drag coefficient is obtained by rearranging equation (2) and inputting the values for Θ.

For airfoils,

$$C_{dc} = \frac{Cdu}{1+0.9\, Cdu\, BR} \tag{3}$$

For blunt shapes,

$$C_{dc} = \frac{Cdu}{1+0.96\, Cdu\, BR} \tag{4}$$

2.4. Existing Correction Method

Jeong et al. [5] presented a new Darrieus turbine correction coefficient based on measured drag coefficients derived at three different blockage ratios. Zaghi et al. [6] looked at a simplified boundary condition that could be utilised in numerical simulations to account for blockage effects in large-scale wind turbine wind tunnel tests. The goal is to create an effective and dependable method for correcting data obtained from

trials with a high blockage coefficient. With the use of a semi-span wing as an example, Haque et al. [7] investigated several aspects of existing correction methods. Standard methods for calculating blockage incorporate various aspects, but they are based on linearized flow theory, such as the source-sink technique and prospective flow assumption, which have inherent constraints, according to the outcomes of analytical relations of standard procedures. The changes are proposed by combining the differences in the solid wall and far-field results in the readings wind tunnel, based on experimental results that have been computed and estimated.

In wind tunnel experiments of tiny horizontal axis wind tunnels, Chen and Liou [11] analysed the effects of tunnel blockage on the turbine coefficient (HAWTS). For tiny TSR under all tested conditions and the analysed blade pitch angle of 25°, the author concludes that no blockage modifications are required. This study also demonstrates that for a BR of 10%, the blockage correction is less than 5%, confirming that no blockage correction for a BR less than 10% in the literature is appropriate. Bešlagić et al. [12] demonstrated how to calculate the correction factor that fixes the recorded wind turbine power in a wind tunnel to remove the blockage effects. To analyse the correction factor of the blockage effects during wind tunnel testing, the authors proposed a blockage correction method in which the wind turbine output performance must be evaluated for multiple blockage ratio values.

Using small scale wind turbine rotor experimental data, Ryi et al. [13] investigated the approach for a blockage effect rectification approach. The improved blockage effect correction method, which has been utilised to process rotor thrust data in closed-circuit and open-circuit wind tunnels, was also explored by the author. Kang et al. [14] investigated a separation blockage-correction method for a wind turbine blade with an airfoil form. For the wall interference correction of the closed test-section wind tunnel, the authors developed a new blockage-correction approach for separated flows around the airfoil of a wind turbine blade. The method was then validated by comparing the corrected results to those of other boundary-condition approaches, both classical and measured.

Ross and Altman [15] discovered that the identical vertical-axis wind turbine concept's wake characteristics and VAWT performance were evaluated at different physical sizes and in two distinct wind tunnels in an attempt to provide some direction on the scaling of the combined impacts on the blockage. Chung and Chen [16] devised a method for calculating the dynamic pressure increment around the model. It has been discovered that using a typical blockage formula, the effect of blockage ratio on the sectional lift and drag coefficients on the centreline of an inclined flat plate can be compensated.

The impact of wind tunnel obstruction on the aerodynamic characteristics of this specific model was discussed by Khalid and Suda [17]. The goal of this study is to establish the best blockage correction method for swimmers' hand aerodynamic research by comparing experimental and numerical data.

The objective of the present paper is to determine the effect of the size and shape of the models on the measurement of the wind tunnel. First, the research will look at how the size and shape of the models' affect drag by understanding the fundamentals of fluid mechanics and aerodynamics and statistically assessing the results. A scope of the study is created for this study that will govern the boundaries and parameters for this study. Streamlined and sphere shapes were the measuring factor for this study. The drag coefficient and pressure were evaluated through CFD simulation and wind tunnel testing. These parameters were used to find the correction coefficient.

3. Research Methodology

The approach used to conduct this research is discussed in this section. The discussion includes justifications for each task as well as the study's configuration.

3.1. Analytical Method

The fundamental equations used in this study were Bernoulli Equation and Continuity Equation. These equations were used in this analysis to calculate the velocity and the pressure distribution on the models' surface. The equations are:

$$P_1 + \frac{1}{2}\rho V_1^2 + \rho g h_1 = P_2 + \frac{1}{2}\rho V_2^2 + \rho g h_2 \quad (5)$$

where ρ is the fluid density, P_1 and P_2 are the pressures at point 1 and point 2, V_1 and V_2 are velocities at point 1 and point 2, g is the acceleration due to gravity, and h_1 and h_2 are the heights of point 1 and point 2. Since the calculations in this analysis are related to the linear flow of fluid, the equation is simplified to equation (6),

$$P_1 + \frac{1}{2}\rho V_1^2 = P_2 + \frac{1}{2}\rho V_2^2 \quad (6)$$

While the Continuity Equation looks as following: -

$$\rho V_1 A_1 = \rho V_2 A_2 \quad (7)$$

where A_1 and A_2 are the areas at point 1 and point 2. Since the fluid velocity is constant inside the wind tunnel, the equation is simplified as followed.

$$V_1 A_1 = V_2 A_2 \quad (8)$$

For this analysis equations (6) and (8) were used simultaneously to find the pressure and velocity at each point of the models. Continuity equation is used to find the velocity and that velocity was substituted in Bernoulli equation to find the pressure at each point. The velocities and pressures found were plotted as a graph and to be used for future calculations.

3.2. Study Cases

3.2.1. Shapes

Based on the scope created for this research, two types of shapes were chosen, which are streamlined and blunt shapes. The streamline shape was the shape of the NACA 0012 airfoil and the blunt shape were the shape of a sphere. For each shape, 3 models with different shapes were designed. The test models were designed and modelled using SolidWorks. To understand more about the effect of the shapes, another two types of shapes were considered for this study. The models were NACA 4412 and NACA 6412 airfoils. NACA 4412 and NACA 6412 are asymmetrical airfoils that were used to study the effect of irregular shapes. A total of three models were considered in this study and the types of shapes are: (i) symmetrical, (ii) asymmetrical, and (iii) blunt.

Figures 1 and 2 show the shapes that were used in this study.

Figure 1. The airfoil-shaped test model.

Figure 2. The sphere-shaped test model.

The profile defines the NACA four-digit wing sections. Maximum camber is expressed as a percentage of the chord in the first digit. The second digit is the maximum camber from the leading edge of the airfoil in tenths of a chord. The last two digits represent the airfoil's maximum thickness as a percentage of the chord.

3.2.2. Sizes

For the symmetric airfoil, NACA 0012 was set as the reference thickness. The thickness of the airfoil is 12% of the length at 30% of the chord. For comparison, NACA 0008 and NACA 0018 airfoils were chosen for this study. NACA 0008 has a thickness of 8% of the chord length where it is smaller in size than NACA 0012 while NACA 0018 has a thickness of 18% of the chord length which is bigger than NACA 0012. For the sphere, the radius of 50 mm, 75mm and 112.5mm were considered.

3.2.3. Velocity

The effect of the velocity was also considered in this study. Few calculations with different inlet velocities were analysed and calculated by using a sphere of 75mm radius and NACA 0012 airfoil.

4. Results and Discussions

This section will discuss the results obtained from the calculations. Note that all the calculations made are ideal. All the calculations were at a 0° angle of attack. The flow was considered inviscid flow for all the calculations, which means the flow has zero viscosity.

4.1. The Effect of the Shapes

The type of the shapes contributes largely to the wind tunnel measurement. Before the wind tunnel testing, the pressure coefficient for each model was calculated manually. Figures 3 and 4 show the velocity and pressure distribution for the three models which are NACA 0012, NACA 4412, and NACA 6412.

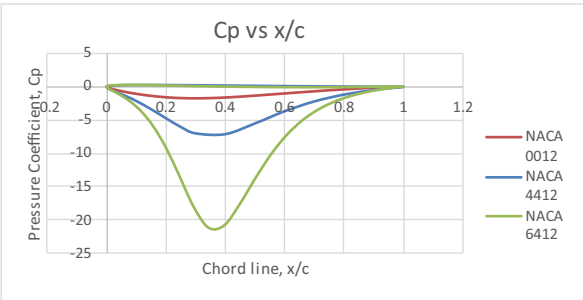

Figure 3. Pressure distribution of NACA 0012, NACA 4412, and NACA 6412 airfoils.

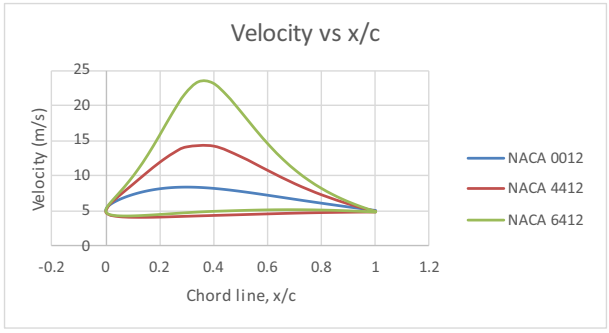

Figure 4. Velocity distribution of NACA 0012, NACA 4412, and NACA 6412 airfoils.

As can be seen in Figure 3 and 4 the velocity distribution and velocity distribution for all the models is different. The pressure distribution graphs plotted were validated with graphs generated by XFOIL software. XFOIL is a tool that allows you to construct and analyse subsonic isolated airfoils interactively. XFOIL can determine the pressure distribution on a 2D airfoil and thus lift and drag characteristics given the coordinates indicating the geometry of the airfoil, Reynolds and Mach numbers. The pressure distribution graph generated for NACA 0012, 4412, and 6412 are shown in Figures 5, 6, and 7. The pressure and velocity distribution calculation results are accurately obtained since the lowest pressure coefficient and highest velocity for all three airfoils is at 0.3 m.

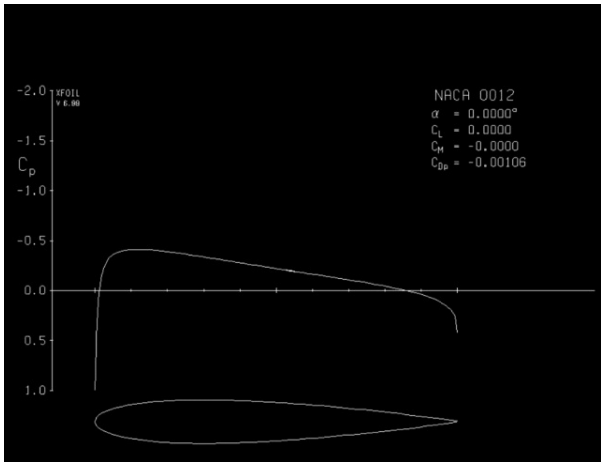

Figure 5. The pressure distribution for NACA 0012 was generated through XFOIL.

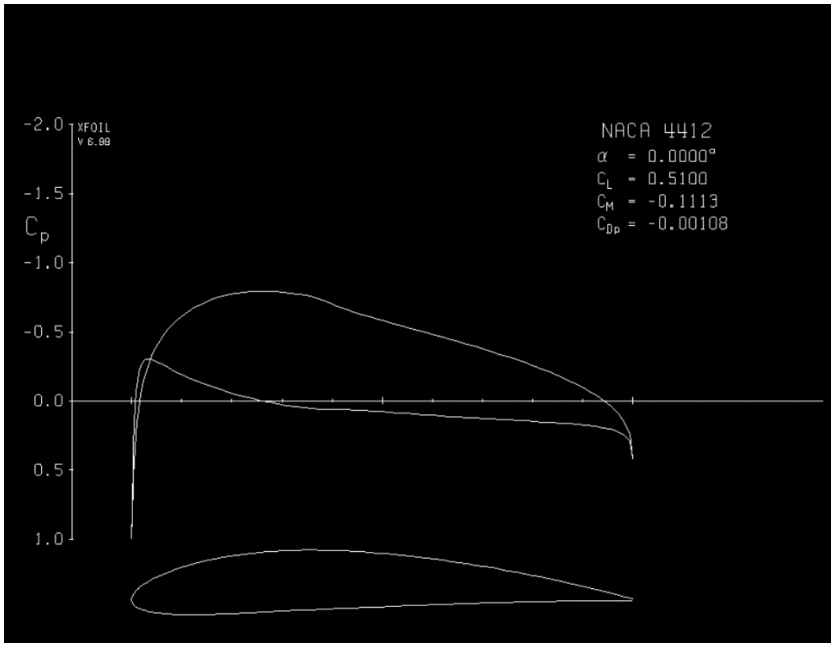

Figure 6. The pressure distribution for NACA 4412 was generated through XFOIL.

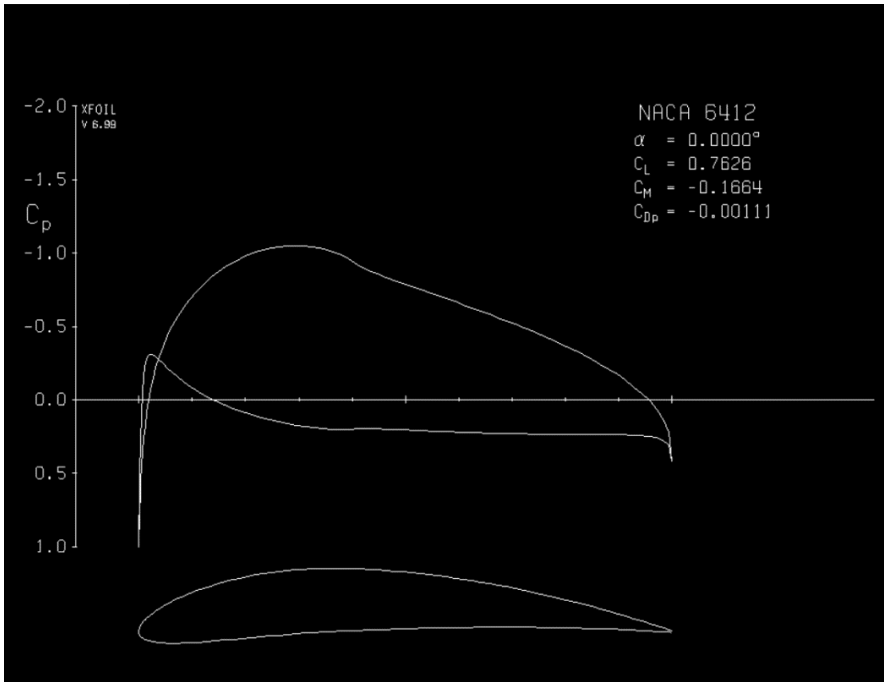

Figure 7. The pressure distribution for NACA 6412 was generated through XFOIL.

4.1.1. Blockage Correction Comparison for Different Shapes

The blockage correction method was applied to all the drag coefficients for all three shapes of airfoils. For this comparison, the reference velocity of 15 m/s was considered. This speed was considered because during the experiment the drag values of the models did not fluctuate much when the readings were taken

repeatedly. The blockage ratio for all three airfoils was constant which is 3%. Blockage ratio is a ratio of the frontal area of the test model to the cross-section of the wind tunnel. These three airfoils were chosen for the study because all the airfoils were in different shapes. NACA 0012 was a symmetrical airfoil, NACA 4412 was a slightly asymmetrical airfoil whereas NACA 6412 was a highly asymmetrical airfoil. Table 1 shows the corrected and uncorrected drag coefficient for NACA 0012, 4412, and 6412.

Table 1. The comparison of reduction in drag coefficient for NACA 0012, NACA 4412, and NACA 6412 airfoils.

Airfoil	Drag Coefficient	Corrected Drag Coefficient	Percentage in Reduction
NACA 0012	0.04228	0.04219	0.11%
NACA 4412	0.06113	0.06103	0.15%
NACA 6412	0.06468	0.06458	0.16%

From Table 1 it can be seen that the reduction percentage is increasing from symmetrical to unsymmetrical. NACA 6412 has the highest drag reduction compared to the other two airfoils. NACA 0012 is an asymmetrical airfoil whereas NACA 4412 and NACA 6412 are asymmetrical airfoils. The maximum camber of all the airfoils evaluated is NACA 6412. Because the flow over the airfoil is on the verge of separation, this increase in drag is attributable to greater values of pressure drag force. In addition, the value of drag for NACA 6412 increases as the height of the airfoil from the ground rises. In the case of NACA 0012, the airfoil has no camber and lower upper surface curvature. As a result, flow separation at the trailing edge is delayed, resulting in the airfoil with the lowest drag of the three.

4.2. Effect of Size

Another aim of this paper is to study the effect of the size of the model. To study this effect, three symmetrical airfoils were considered. The airfoils were NACA 0008, NACA 0012, and NACA 0018. All three airfoils have the same shapes but different thicknesses. Figures 8 and 9 shows the comparison of velocity and pressure distribution for all three airfoils.

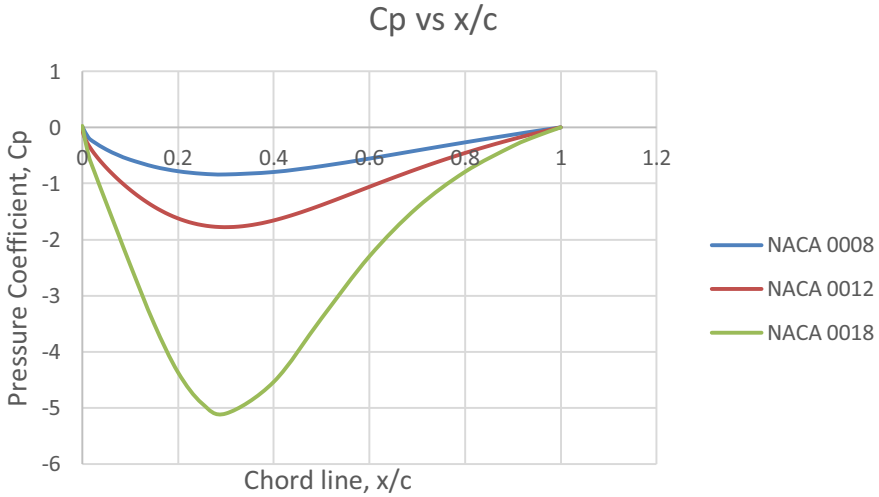

Figure 8. Pressure distribution of NACA 0008, NACA 0012, and NACA 0018 airfoils.

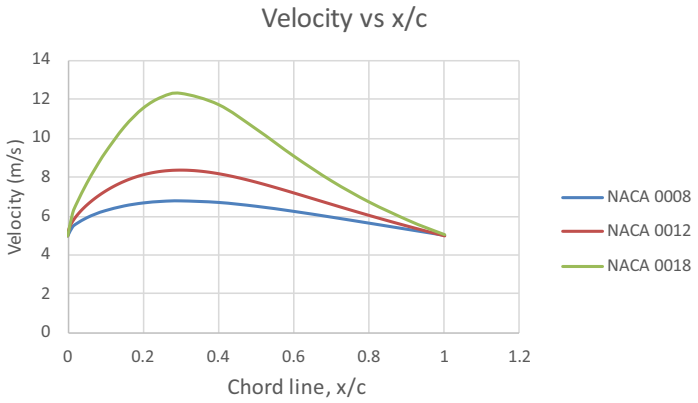

Figure 9. Velocity distribution of NACA 0008, NACA 0012, and NACA 0018 airfoils.

Based on Figures 8 and 9, the thicker the airfoil the higher the velocity and the lower the pressure distribution on the airfoils. So, the size of the shapes will affect the wind tunnel measurement.

4.2.1. Blockage Correction Comparison for Different Sizes

The blockage correction method was applied to all the drag coefficients for all three sizes of the airfoils. For this comparison, the reference velocity of 15m/s was considered. The blockage ratio for all three airfoils was varied since all the airfoils have different thicknesses. The shape of the airfoils was kept constant where all the airfoils were symmetrical. Table 2 shows the corrected and uncorrected drag coefficient for NACA 0008, 0012, and 0018.

Table 2. The comparison of reduction in drag coefficient for NACA 0008, NACA 0012, and NACA 0018 airfoils.

Airfoil	Drag Coefficient	Corrected Drag Coefficient	Blockage Ratio	Percentage in Reduction
NACA 0008	0.041635	0.04160	2%	0.07%
NACA 0012	0.042238	0.04219	3%	0.11%
NACA 0018	0.042280	0.04220	4.5%	0.19%

From Table 2, a graph of percentage in reduction against blockage ratio was plotted as shown in Figure 10. The plotted graph was used to derive the correction coefficient equation.

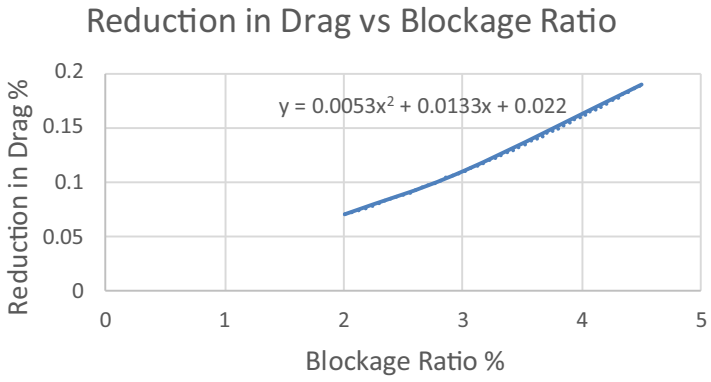

Figure 10. Drag reduction against blockage ratio for airfoils.

From the graph shown in Figure 9, a generalized equation to estimate the blockage correction coefficient, y can be used to find blockage correction for airfoils. The following correction coefficient as a function of the blockage ratio was obtained.

$$y = 0.005Br^2 + 0.0133Br + 0.022 \quad (9)$$

The same blockage correction method was applied for all the sphere sizes. As the airfoils, the reference velocity of 15 m/s was considered. The blockage ratio for all the spheres was varied since all the spheres have a different radius. Table 3 shows the corrected and uncorrected drag coefficient for the spheres of the different radius of spheres.

Table 3. Corrected and uncorrected drag for the different blockage ratios of the spheres.

Radius of the Spheres (mm)	Drag Coefficient	Corrected Drag Coefficient	Blockage Ratio	Percentage in Reduction
25	0.0144	0.0144	0.694%	0%
50	0.034066	0.03397	8.7%	0.28%
75	0.078272	0.07713	19.6%	1.45%
112.5	0.066811	0.06533	35.3%	4.09%

From Table 3, a graph of percentage in reduction against blockage ratio was plotted as shown in Figure 11. The plotted graph was used to derive the correction coefficient equation.

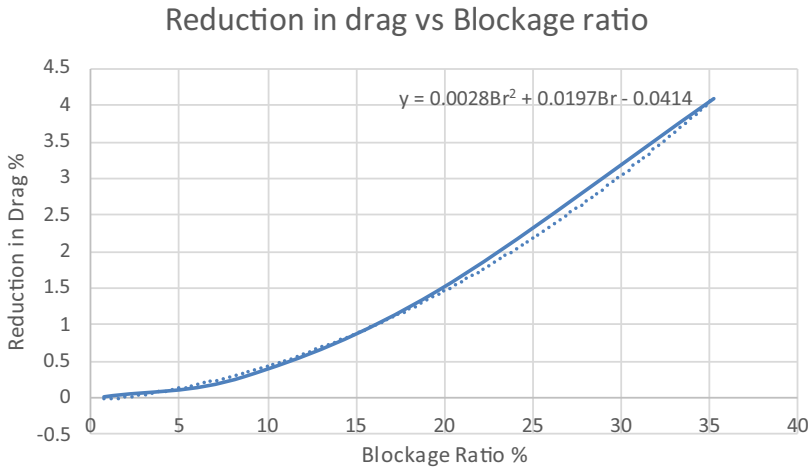

Figure 11. The graph of drag reduction against blockage ratio for spheres.

From the graph shown in Figure 10, a generalized equation to estimate the blockage correction coefficient, y can be used to find blockage correction for spheres. The following correction coefficient as a function of the blockage ratio was obtained.

$$y = 0.0028Br^2 + 0.0197Br - 0.0414 \quad (10)$$

4.3. Effect of Velocity

The inlet velocity of the wind tunnel also contributes to the pressure and velocity distribution of the models. The pressure and velocity distribution on a sphere model was calculated with varying inlet velocities, which

are 5 m/s, 10 m/s, 15 m/s, 20 m/s, and 25 m/s. Figures 12 and 13 show the results of varying velocities tested with the model.

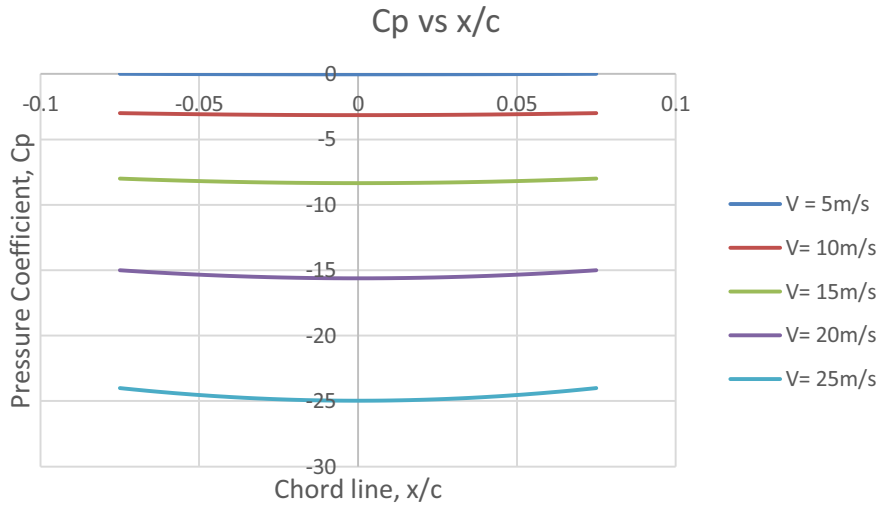

Figure 12. Pressure distribution of the sphere on varying inlet velocity

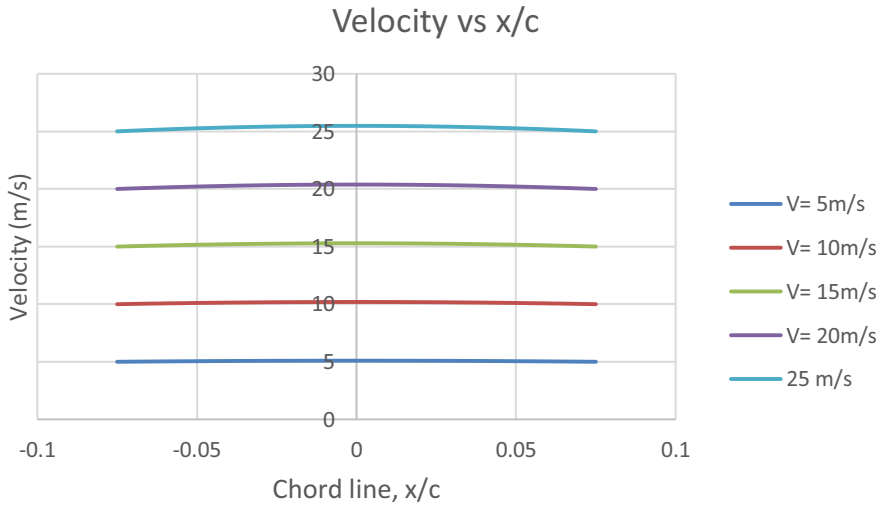

Figure 13. Pressure distribution of the sphere on varying inlet velocity.

Regardless of the velocity, the trends of pressure distribution and velocity distribution were similar. The maximum velocity and lowest pressure on the sphere are at 75mm since 75mm is the maximum radius of the sphere.

The same trend follows when NACA 0012 airfoil is tested with different inlet velocities. The same calculations were conducted on the airfoil. Figures 14 shows the results of varying velocities tested with the model.

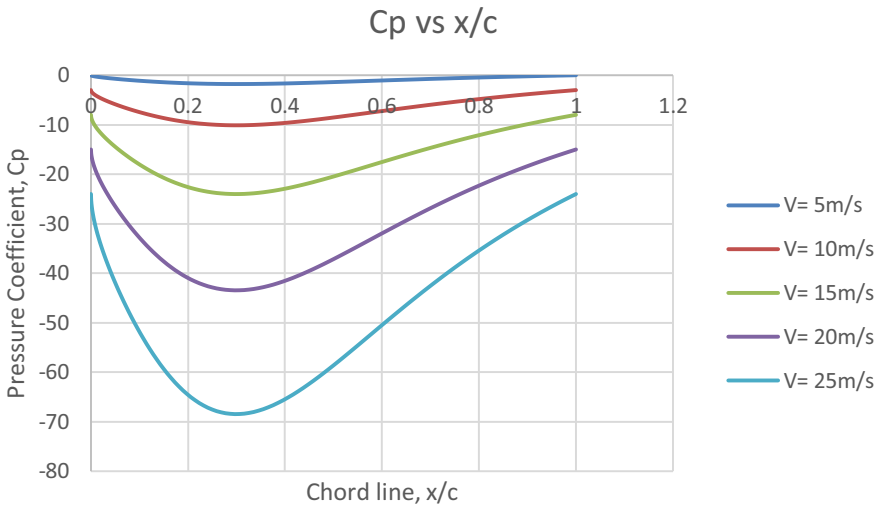

Figure 14. Pressure distribution of NACA 0012 with varying inlet velocity.

Similar to the sphere's test, the pressure distribution decreases, and the velocity distribution increases when the inlet velocity increases. Regardless of the velocity, the trend remains the same for all the tests. The highest velocity and lowest pressure are at the maximum thickness, which is at 30% of the chord line.

5. Conclusion and Recommendations

This research quantitatively evaluates the blockage effect that occurs during the wind tunnel test of spheres and airfoils. Airfoils and spheres with different types of shapes and sizes were installed in the wind tunnel to study the effects of both parameters on the wind tunnel surfaces. From the study, it is concluded that the models that have a blockage ratio lower than 16% have no significant blockage effect on TLWT reading. Hence, the blockage effect created by these models is negligible, whereas, models with a blockage ratio of 16% and higher induce a non-negligible blockage effect that has to be corrected. A correction coefficient to correct the blockage effect by both shapes has been derived in this study.

References

[1] Eltayesh A, Hanna M B, Castellani F, Huzayyin A S, El-Batsh H M, Burlando M and Becchetti, M 2019 Effect of wind tunnel blockage on the performance of a horizontal axis wind turbine with different blade number *Energies* **12(10)** 12
[2] Anthoine J, Olivari D and Portugaels D 2009 Wind-tunnel blockage effect on drag coefficient of circular cylinders *Wind and Struct.* **12(6)** 541-51
[3] Al-Obaidi A S M and Yang L H 2017 Numerical and experimental assessment of velocity with/without model inside Taylor's wind tunnel test section *The 5th Engineering Undergraduate Research Catalyst* Taylor's University, Subang Jaya Malaysia
[4] Nordin N, Abdul Karim Z A, Othman S and Raghavan V R 2012 Design and development of low subsonic wind tunnel for turning diffuser application *Adv. Mater. Res.* **614-615** 586-91
[5] Jeong H, Lee S and Kwon S D 2018 Blockage corrections for wind tunnel tests conducted on a Darrieus wind turbine *J. Wind Eng. Ind. Aerodyn.* **179** 229-39
[6] Zaghi S, Muscari R and Mascio A D 2016 Assessment of blockage effects in wind tunnel testing of wind turbines *J. Wind Eng. Ind. Aerodyn.* **154** 1-9.

[7] Haque A U, Asrar W, Omar A A, Sulaeman E and Ali M J S 2016 Comparison of data correction methods for blockage effects in semispan wing model testing *EPJ Web of Conf.* **114**, 02129
[8] Takeda K and Kato M 1992 Wind tunnel blockage effects on drag coefficient and wind-induced vibration *J. Wind Eng. Ind. Aerodyn.* **42(1-3)** 897-908
[9] Maskell E C (1963) A theory of the blockage effects on bluff bodies and stalled wings in a closed wind tunnel. No. ARC-R/M-3400; Aeronautical Research Council: London, UK.
[10] Elfmark O, Reid R and Bardal L M 2020 Blockage correction and Reynolds number dependency of an alpine skier: A comparison between two closed-section wind tunnels *Proc.* **49(1)** 19
[11] Chen T Y and Liou L R Blockage corrections in wind tunnel tests of small horizontal-axis wind turbines *Exp. Therm Fluid Sci.* **35(3)** 565-69
[12] Bešlagić E, Lemeš S and Hadžikadunić F 2020 Procedure for determining the wind tunnel blockage correction factor *New Technol. Dev. Appl.* ***III*** 331-39
[13] Ryi J, Rhee W, Hwang U C and Choi J S 2015 Blockage effect correction for a scaled wind turbine rotor by using wind tunnel test data *Renewable Energy* **79** 227-35
[14] Kang S H, Shin E S, Ryu K W and Lee J s 2013 Separation blockage-correction method for the airfoil of a wind turbine blade *J. Mech. Sci. Technol.* **27** 1321-27
[15] Ross I and Altman A 2011 Wind tunnel blockage corrections: Review and application to Savonius vertical-axis wind turbines *J. Wind Eng. Ind. Aerodyn.* **99(5)** 523-38
[16] Chung K M and Chen Y J 2016 Effect of high blockage ratios on surface pressures of an inclined flat plate *J. Eng. Archit.* **4(2)** 82-92
[17] Khalid U B and Suda J M 2020 Comparative study of wind tunnel blockage correction methods for bluff body aerodynamics (Swimmer's hand model) *MSc Thesis* Budapest University of Technology and Economics Faculty of Mechanical Engineering